

Remarks on the non-equilibrium effects and collision dynamics in heavy-ion collisions

Yogesh K. Vermani and Mandeep Kaur

Department of Physics, Panjab University, Chandigarh -160 014, India

(Dated: November 15, 2018)

We study the beam energy dependence of equilibration process and space-time characteristics of participant and spectator matter. For this, we simulated the semi-central collisions of $^{40}\text{Ca} + ^{40}\text{Ca}$ at incident energies of 400, 600 and 1000 AMeV within the *quantum molecular dynamics* (QMD) approach. Our numerical calculations based on the molecular dynamics approach show that incident energy of the projectile influences the reaction observables drastically. The effect is more visible for transverse expansion of the nuclear matter and transparency behavior. The degree of thermalization of participant matter, however, remains independent of the incident energy. The characteristics of the trajectories followed by the nucleons suffering maximal and minimal binary collisions are also analyzed.

PACS numbers: 25.70.-z, 25.75.Ld, 24.10.Lx

I. INTRODUCTION

The simulation of heavy-ion collisions at intermediate energies has always played a pivotal role in understanding the reaction mechanism [1–7], nature of nucleon-nucleon (n - n) interactions, as well as thermalization achieved by the nuclear system [8–10]. Similar efforts are also made at lower tail of the incident energy where fusion and cluster-decay processes are dominant [11–14]. The choice of various transport codes, beyond doubt, provides a unique platform to study the properties of hot & dense nuclear matter formed during these collisions. In these transport models, one starts from the well separated projectile and target nuclei and then evolves towards non-equilibrium stage due to the overlapping of two Fermi spheres with large relative momentum. The dynamics of heavy-ion (HI) collision can be interpreted in terms of useful reaction observables such as collective flow [15–18], multifragment-emission [1, 17, 19], temperature and entropy production [17], momentum anisotropy, subthreshold particle production as well as elliptical flow [8, 17, 19–22].

The different studies have shown that for a given colliding geometry, the final particle abundances are sensitive towards the incident energy of the projectile [23, 24]. These theoretical predictions, however, were largely based on the assumption of thermal equilibrium of the nuclear system. It may be emphasized that at SIS energies, particles are produced in highly non-equilibrium situation much different from the saturation characteristics of the normal nuclear matter [25]. Recently, the BUU simulation of $^{197}\text{Au} + ^{197}\text{Au}$ collisions at 1 AGeV reported that spectator matter evolution is strongly influenced by the compression and expansion of the participant matter [26]. The transverse expansion of the spectator matter is found to be sensitive towards the nuclear incompressibility of the participant zone [26]. At relativistic bombarding energies, the spectator matter fragmentation [5, 6] and its universality characteristics [1, 27–29] have been extensively studied in recent literature. As far as participant matter physics is concerned, extensive study

has been made in the past to infer the properties of hot and dense participant zone [5, 8, 30–33]. Unfortunately, excited nuclear matter under the extreme conditions of temperature and density exists for a very short duration. This makes it difficult to extract information about the nuclear forces and reaction dynamics in experiments. For instance, nuclear matter at nuclear density $\rho > 1.5\rho_0$ lasts for the time span less than 20 fm/c [22, 34]. It is interesting to study the behavior of participant matter and its response towards the evolution of the spectator matter during the collision process. This study also bears relevance due to its relation with the nuclear equation of state (EoS) and flow systematics.

During the collision process, different kinds of interactions are at work which are important in their own [35, 36]. One is also interested to know behavior of nucleons in the presence of other nucleons in the surroundings. From the trajectories traversed by the nucleons in phase space, one can gain important information on the nature of the hadronic forces as well. In the present work, we aim to analyze the reaction dynamics in the semicentral collisions of $^{40}\text{Ca} + ^{40}\text{Ca}$ at incident energies of 400, 600 and 1000 AMeV respectively. We shall also examine the behavior of nucleons facing maximal and minimal number of collisions via stopping and trajectories followed in the phase space during the collision process.

For the simulation of heavy-ion reactions, we shall utilize the *quantum molecular dynamics* (QMD) model [1, 5, 6, 19, 37–39] as primary transport theory which is described in II. Section III deals with the calculations and illustrative results, which are summarized in section IV.

II. THE MODEL

The quantum molecular dynamics is an N-body theory that simulates the heavy-ion reactions at intermediate energies on event by event basis. This is based on a molecular dynamics picture where nucleons interact via two and three-body interactions. The explicit two and

three-body interactions preserve the fluctuations and correlations which are important for N -body phenomenon. In this approach, each single nucleon of the two colliding nuclei is described by a Gaussian wave packet in momentum and coordinate space. The centroids of these Gaussian wave packets propagate in coordinate (\mathcal{R}_3) and momentum (\mathcal{P}_3) spaces in accordance with the classical equations of motion:

$$\dot{\mathbf{p}}_i = -\frac{\partial U_i}{\partial \mathbf{r}_i}, \quad \dot{\mathbf{r}}_i = \frac{\mathbf{p}_i}{\sqrt{\mathbf{p}_i^2 + m_i^2}} + \frac{\partial U_i}{\partial \mathbf{p}_i}. \quad (1)$$

In the quantum molecular dynamics approach, nucleons move along classical trajectories and undergo stochastic scattering. Stochastic means that scattering amplitude doesn't relate the scattering angle with the impact parameter in a unique way like the collision of classical billiard balls. Collisions are Pauli blocked if scattered nucleons enter the phase space region which is already occupied. The local Skyrme interaction used here, consists of two and three-body n - n interactions:

$$V_{ij}^{loc} = t_1 \delta(\mathbf{r}_i - \mathbf{r}_j) + t_2 \delta(\mathbf{r}_i - \mathbf{r}_j) \delta(\mathbf{r}_i - \mathbf{r}_k). \quad (2)$$

This interaction (2) is supplemented with a long-range Yukawa and an effective charge Coulomb interaction parts [37]:

$$V_{ij}^{Yuk} = t_3 \frac{\exp\{-|\mathbf{r}_i - \mathbf{r}_j|\}/\mu}{|\mathbf{r}_i - \mathbf{r}_j|/\mu} \quad (3)$$

$$V_{ij}^{Coul} = \frac{Z_i \cdot Z_j e^2}{|\mathbf{r}_i - \mathbf{r}_j|} \quad (4)$$

Z_i, Z_j are the effective charge of baryons i and j . In QMD model, one neglects the isospin dependence of the interaction. All nucleons in a nucleus are assigned the effective charge $Z = \frac{Z_T + Z_P}{A_T + A_P}$ [37]. The long-range Yukawa force is necessary to improve the surface properties of the interaction. The parameters μ, t_1, t_2, t_3 in Eqs (2), (3) and (4) are adjusted and fitted so as to achieve the correct binding energy and mean square root values of the radius of the nucleus [37]. The Skyrme-type potential can be generalized to density dependent form as [37, 39]:

$$U^{Skm} = \alpha \left(\frac{\rho}{\rho_0} \right) + \beta \left(\frac{\rho}{\rho_0} \right)^\gamma, \quad (5)$$

with α and β as free parameters. These are fixed by the ground state properties of normal nuclear matter. The third parameter γ allows to fix the incompressibility of the nuclear matter. The two parameterizations are commonly used namely 'soft' and 'hard' corresponding to different incompressibilities of the nuclear matter. We shall use here a 'soft' equation of state with incompressibility $K=200$ MeV.

III. NUMERICAL CALCULATIONS AND DISCUSSION

First of all, we study the reaction observables for the semicentral collisions of $^{40}\text{Ca} + ^{40}\text{Ca}$ at incident ener-

gies of 400, 600 and 1000 AMeV. Figure 1 displays the model calculations of the average nuclear density ρ^{avg} , collision rate dN_{coll}/dt , directed transverse momentum $\langle p_x^{dir} \rangle$ and momentum anisotropy ratio $\langle R_{iso} \rangle$ of the participant matter obtained for the reaction $^{40}\text{Ca} + ^{40}\text{Ca}$ at a 'reduced' impact parameter $b/b_{max}=0.3$. The nuclear matter density is calculated as:

$$\rho^{avg} = \left\langle \frac{1}{N} \sum_{i=1}^N \sum_{j>i}^N \frac{1}{(2\pi L)^{3/2}} e^{-(\mathbf{r}_i(t) - \mathbf{r}_j(t))^2 / 2L} \right\rangle, \quad (6)$$

In our approach, the average nuclear matter density ρ^{avg} is calculated in a volume cell of $2 fm$ with center located at the point where two nuclei initially touch each other in c.m. frame. As expected, one obtains maximum central density at the highest considered energy of 1000 AMeV. A similar behavior can be seen for the allowed collision rate dN_{coll}/dt . The directed transverse momentum p_x^{dir} is another important quantity describing the transverse expansion of the nuclear matter. It is defined as:

$$\langle p_x^{dir} \rangle = \frac{1}{N} \sum_{i=1}^N \text{sign}(y_i) \cdot p_x(i), \quad (7)$$

with $p_x(i)$ as x -component of momentum. y_i is the rapidity of i^{th} particle evaluated as:

$$y_i = \frac{1}{2} \ell n \frac{E(i) + p_z(i)c}{E(i) - p_z(i)c}. \quad (8)$$

Here $E(i)$ and $p_z(i)$ are the total energy and the longitudinal momentum of the i^{th} particle, respectively. Interestingly at the start of the reaction (for $t < 20 fm/c$), $\langle p_x^{dir} \rangle$ turns negative (See figure 1(c)). This happens due to attractive interaction between two nuclei in the beginning. After the two nuclei collide, strong repulsion takes place in the overlap region. As a result, transverse flow turns positive and saturates finally. The time evolution of the transverse momentum transfer depicts that it starts to have finite value when nuclear matter is still interacting and density is quite high. Beyond 40 fm/c, the transfer of momentum in transverse direction is not much altered, indicating the expansion of the nuclear matter in transverse direction has ceased. One clearly obtains more transverse expansion at 1000 AMeV as compared to lower incident energies. It means that nucleons with larger relative momenta are directed into the transverse direction with higher momenta. It is worth interesting to compare the degree of equilibrium attained by the participant zone at these bombarding energies. We display in the bottom panel of figure 1, the momentum anisotropy ratio $\langle R_{iso} \rangle$ for the participant zone, calculated as [8, 22]:

$$\langle R_{iso} \rangle = \frac{\sqrt{\langle p_x^2 \rangle} + \sqrt{\langle p_y^2 \rangle}}{2\sqrt{\langle p_z^2 \rangle}}. \quad (9)$$

To select momentum anisotropy due to participant zone, we impose the condition $(-0.5y_{beam} \leq y \leq 0.5y_{beam})_{c.m.}$

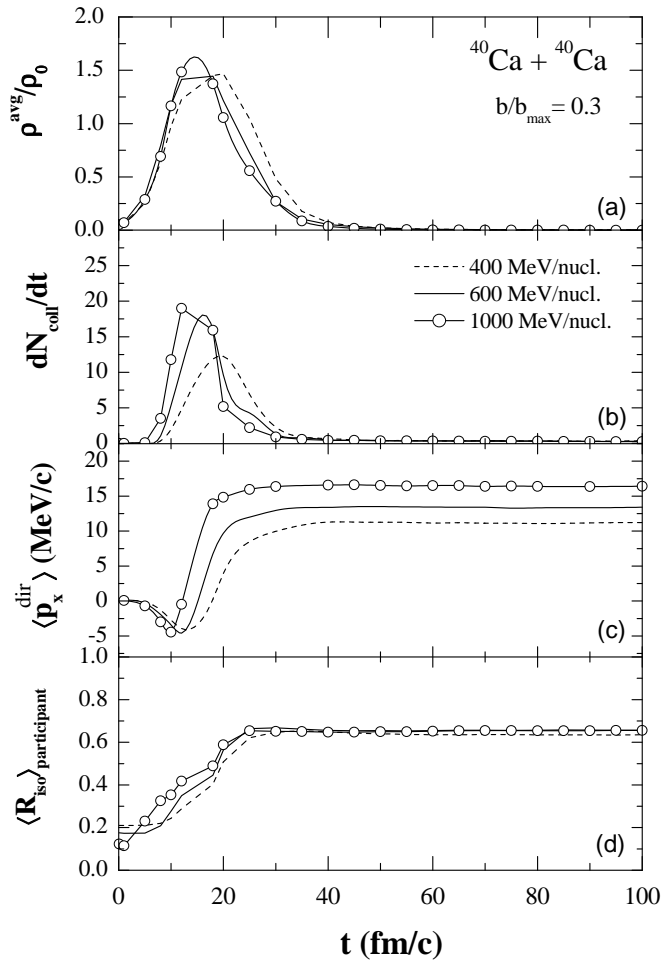


FIG. 1. The time evolution of $^{40}\text{Ca}+^{40}\text{Ca}$ reaction at incident energies of 400, 600 and 1000 AMeV and at ‘reduced’ impact parameter $b/b_{max}=0.3$. Results are shown here for: (a) mean central density ρ^{avg}/ρ_0 ; (b) average collision rate dN_{coll}/dt ; (c) directed transverse momentum $\langle p_x^{dir} \rangle$; and (d) anisotropy ratio $\langle R_{iso} \rangle$ of the participant zone.

on the event rapidity. The application of this cut allows to exclude spectator like components. The full equilibrium corresponds to $\langle R_{iso} \rangle$ value close to 1. One can see that equilibration of the participant matter gets saturated shortly after decompression. This is also the time when spectator components start departing from the hot interaction zone and we have the uniform directed transverse momentum, thereafter. This shows that spectator and participant components hardly interact after this time. However full equilibrium is not attained even at 1000 AMeV. Interestingly, at all three incident energies considered here, the anisotropy ratio $\langle R_{iso} \rangle$ converge to same value. This indicates that equilibration of participant matter in semicentral Ca+Ca collisions takes place to nearly same extent, irrespective of the incident energy. These findings are supported by the fact that in Plastic Ball experiments, nearly the same baryonic entropy

is produced [40] at different bombarding energies. The R_{iso} value is not much altered unlike the mean directed transverse momentum $\langle p_x^{dir} \rangle$. It may be mentioned that momentum anisotropy ratio is still less than 1 with approximately 25 % anisotropy in momentum distribution. This also indicates that surrounding spectator components has strong influence on the evolution of participant matter. As a result, one can’t have always full stopping and thermalization even for the central overlap region. As far as peripheral collisions are concerned, the participant component, therefore, retains the *transparency* character in the longitudinal direction, and momentum distribution of nucleons is far from that of thermalized source. This also shows that nucleons are in quite highly non-equilibrium environment that can not be described with single fireball model [41], or oversimplified hydrodynamical prescription [42].

In 2, we display the momentum distribution of nucleons for the single event of Ca+Ca collision obtained at 100 fm/c. The two dimensional plane in the figure corresponds to longitudinal momentum p_z versus total transverse momentum $p_T (= \sqrt{p_x^2 + p_y^2})$. Our model predictions clearly show the impact of bombarding energy on transverse expansion of the nuclear matter. This leads to increase in $\langle p_x^{dir} \rangle$ with incident energy, as mentioned earlier. One can observe appreciable *transparency* character of the nuclear matter in longitudinal direction. This happens due to the fact total number of n - n collisions taking place in the medium are not able to keep the pace with transverse expansion. Owing to this phenomenon, we have less equilibrated matter with $\langle R_{iso} \rangle$ value slightly less than unity. Next, we try to understand the stopping pattern of the nucleons facing maximal and minimal number of collisions by analyzing the variation in their rapidities at different time steps. Figure 3 shows the variation of normalized rapidity y/y_{beam} of single spectator nucleon, facing zero collision ($n_{coll} = 0$) and participant nucleon ($n_{coll} = 14$) followed for the time span of 100 fm/c. We have displaced here the symbols corresponding to same rapidity bin but obtained at different time steps along the y-axis, though all these points have same probability of occurrence. This is done to make the variation in the longitudinal rapidity with time more vivid. The numbers in the boxes imply the time interval for which the nucleon stays in particular rapidity bin. At the start of the reaction, both particles are seen at projectile beam rapidity y_{beam} . With advent of the collision process, participant nucleons (suffering 14 collisions) are stopped around *mid-rapidity* with $y/y_{beam}=0.25$. On the other side, the spectator nucleons (as shown in the upper panel) still stay in the higher rapidity regime with $y/y_{beam}=1$. Again, one can also notice that participant nucleon suffers more fluctuations in its longitudinal rapidity. The spectator particle, however, remains in the projectile’s rapidity regime for most of the time. The temperature reached in HI reactions at intermediate energies can be as high as 70-80 MeV [22]. Nucleons feeling such hot environment would behave differently than

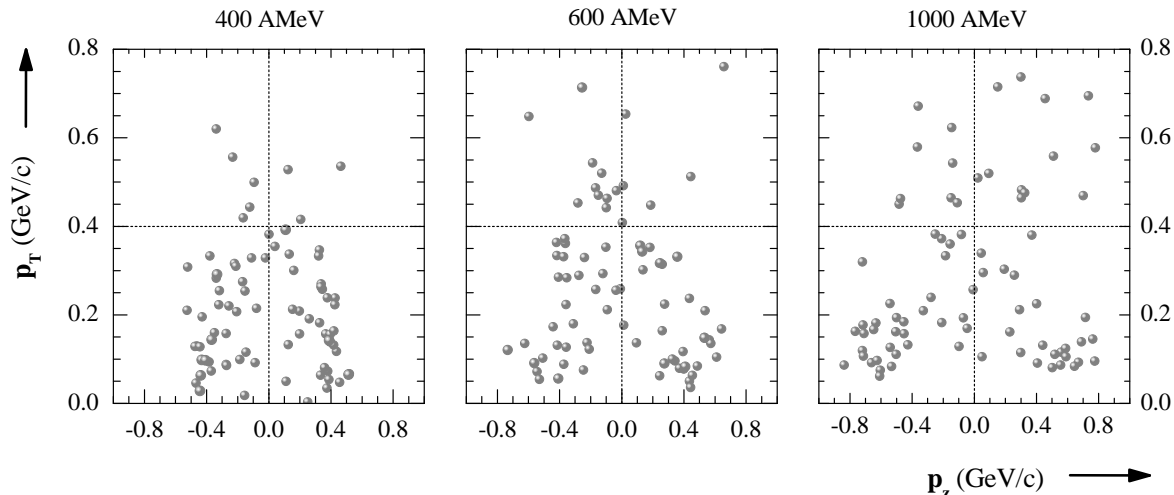


FIG. 2. The plots of transverse momentum p_T vs longitudinal momentum p_z of the nucleons obtained in a single event of Ca+Ca collision at 400 (left), 600 (middle), and 1000 (right) AMeV and with $b/b_{max}=0.3$. Momentum distribution of nucleons has been calculated at 100 fm/c.

those found in relatively cold spectator zones. It is interesting to follow the space-time characteristics of these nucleons facing maximal (*i.e.* participants) and minimal (*i.e.* spectators) number of collisions. This study can be of importance to understand characteristics of hot participant matter and hadronic interactions as well. For this study, we randomly choose the nucleons from target and projectile in ^{40}Ca (400 AMeV)+ ^{40}Ca collision. The left panel of 4, shows the time evolution of total momentum P_n of individual spectator nucleons (P_{15} , P_{32} , P_{47} , P_{60}). Similarly, the evolution of participant nucleons (P_9 , P_{39} , P_{49} , P_{71}) facing maximal collisions is shown in the right panel.

The particles behaving like spectators aren't expected to feel the hot environment even during the violent stage of the reaction. Owing to this, one obtains minimum fluctuations in the particle's momentum during the collision process. On the other hand, participant nucleons facing maximal number of collisions, feel the hot environment as indicated by continuously change in their momenta during the collision. The participant nucleons, therefore, suffer more number of fluctuations in momentum space. We also aim to analyze the behavior of these nucleons in coordinate space. Figure 5 displays the trajectories of these nucleons in x - z plane followed for the time span of 300 fm/c starting from the initial contact between the projectile and target nuclei. Since nucleons facing minimal number of collisions are knocked-out quite earlier, they traverse nearly straight line paths in \mathcal{R}_3 -space. Contrary to this, the participant nucleons (as shown in

the right panel) face large fluctuations along their trajectories as expected. These particles remain in the hot zone for appreciably long time unlike spectator nucleons which are knocked-out of the reaction zone during the early stage of the reaction.

IV. SUMMARY

Summarizing, we have presented an exclusive analysis of the semicentral Ca+Ca reactions at incident energies 400, 600 and 1000 AMeV within quantum molecular dynamics approach. Our findings showed that incident energy of the projectile strongly influences the observables *viz.* average nucleonic density, allowed collision rate as well as the transverse expansion of nuclear matter. Further, the transparency effect in the nuclear medium also seems to get enhanced with the incident energy. Interestingly, the degree of equilibrium achieved by the participant zone remains insensitive to the range of projectile energies considered in this work. The full equilibration is not always there even for the participant zone. A detailed analysis of trajectories traversed by the nucleons depicted that spectator and participant nucleons behave differently in the coordinate and momentum space. The nucleons facing maximal collisions *i.e.* participant nucleons suffered extensive fluctuations in their momentum and spatial coordinates. The spectator nucleons, on other hand, depart from the hot reaction zone quite earlier and traverse nearly the straight line trajectories.

[1] Vermani Y K, Goyal S and Puri R K 2009 Phys. Rev. C **79** 064613

[2] Vermani Y K and Puri R K 2009 *Europhys. Lett.* **85** 62001

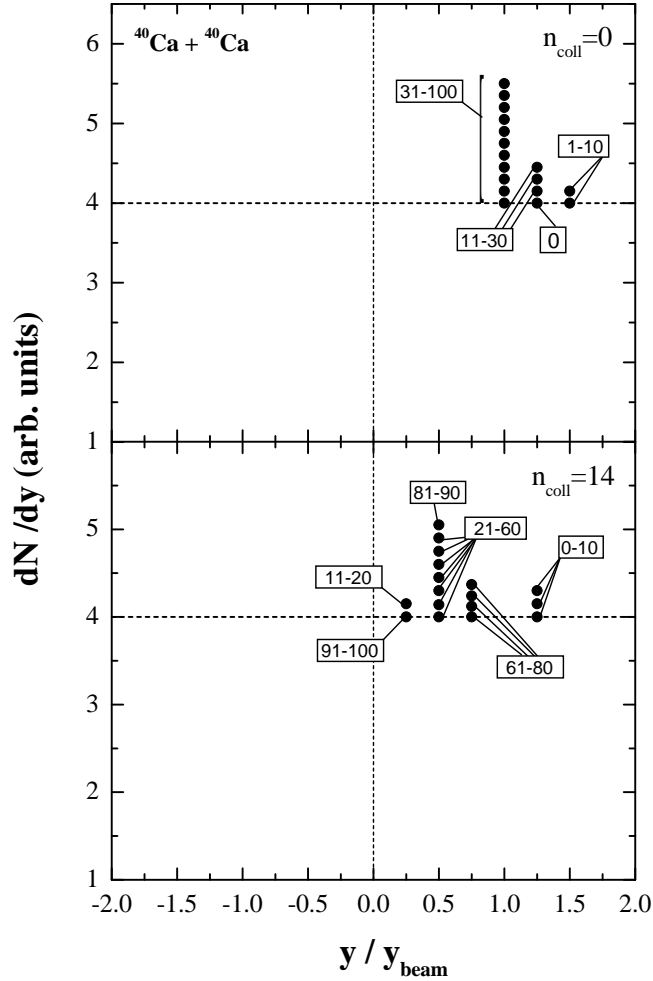


FIG. 3. The rapidity distribution dN/dy vs normalized rapidity y/y_{beam} in the nucleus-nucleus c.m. frame for the evolution of single spectator (top) and participant (bottom) nucleons. Results are shown here for the single event of Ca (40 AMeV)+ Ca collision with $b/b_{max}=0.3$.

- [3] Vermani Y K and Puri R K 2010 *J. Phys. G: Nucl. Part. Phys.* **37** 015105
- [4] Vermani Y K and Puri R K 2010 *Nucl. Phys. A* DOI: 10.1016/j.nuclphysa.2010.07.005
- [5] Wu H L et al 2010 *Phys. Rev. C* **81** 047602; Sood A D and Puri R K 2009 *Phys. Rev. C* **79** 064618
- [6] Fèvre A Le et al 2009 *Phys. Rev. C* **80** 044615; Xu Chang and Li Bao-An 2010 *Phys. Rev. C* **81** 044603
- [7] Hartnack Ch, Oeschler H and Aichelin J 2006 *Phys. Rev. Lett.* **96** 012302
- [8] Dhawan J K, Dhiman N K, Sood A D and Puri R K 2006 *Phys. Rev. C* **74** 057901
- [9] Moretto L G and Wozniak G J 1993 *Annu. Rev. Nucl. Part. Sci.* **43** 379.
- [10] Fuchs C, Lehmann E, Puri R K, Sehn L, Faessler A and Wolter H H 1996 *J. Phys. G: Nucl. Part. Phys.* **22** 131.
- [11] Puri R K and Gupta R K 1992 *Phys. Rev. C* **45** 1837; Puri R K and Gupta R K 1992 *J. Phys. G: Nucl. Part.*

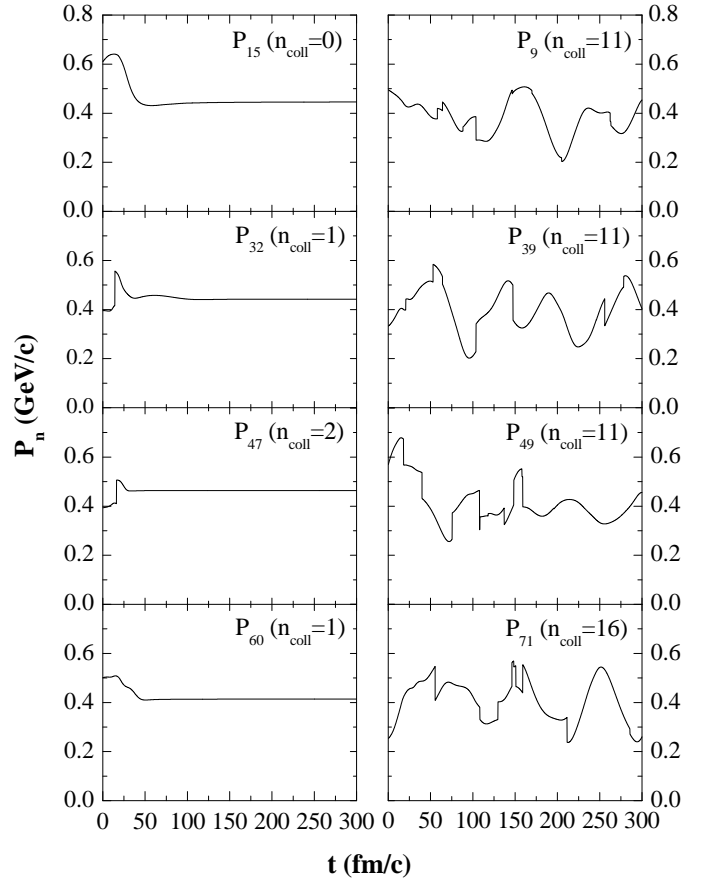


FIG. 4. The time evolution of total momentum P_n (in GeV/c) of randomly chosen nucleons facing minimal collisions (left) and maximal collisions (right).

- Phys.* **18** 903; Malik S S et al 1989 *Pramana J. Phys.* **32** 419; Puri R K et al 1989 *Europhys. Lett.* **9** 767; Arora R et al 2000 *Eur. Phys. J. A* **8** 103; Puri R K et al 2005 *Eur. Phys. J. A* **23** 429.
- [12] Puri R K, Chattopadhyay P and Gupta R K 1991 *Phys. Rev. C* **43** 315; Puri R K et al 1998 *Eur. Phys. J. A* **3** 277.
- [13] Dutt I and Puri R K 2010 *Phys. Rev. C* **81** 044615; Dutt I and Puri R K 2010 *Phys. Rev. C* **81** 047601.
- [14] Shorto J M B, Gomes P R S, Lubian J, Canto L F and Lotti P 2010 *Phys. Rev. C* **81** 044601.
- [15] Lehemann E, Faessler A, Zipprich J, Puri R K and Huang S W 1996 *Z. Phys. A* **355** 55. Kumar S, Sharma M K, Puri R K, Singh K P and Govil I M 1998 *Phys. Rev. C* **58** 3494
- [16] Magestro D J, Bauer W and Westfall G D 2000 *Phys. Rev. C* **62** 041603(R); Sood A D and Puri R K 2004 *Phys. Rev. C* **70** 034611.
- [17] Wolf Gy, Barz H W and Kämpfer B 1999 *Prog. Part. Nucl. Phys.* **42** 157
- [18] Dhawan J K and Puri R K 2006 *Phys. Rev. C* **74** 054610
- [19] Puri R K, Hartnack Ch and Aichelin J 1996 *Phys. Rev. C* **54** R28; Puri R K and Aichelin 2000 *J. Comput. Phys.*

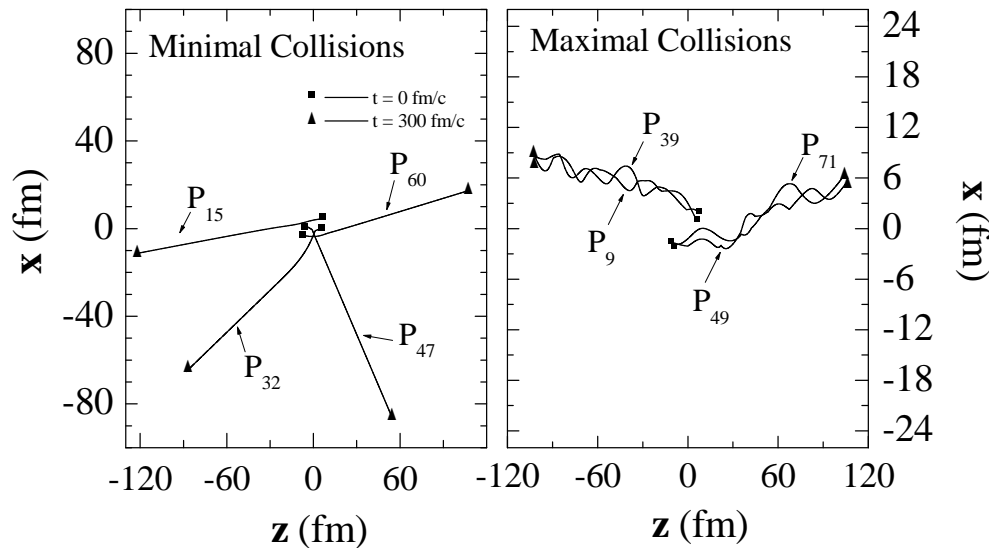


FIG. 5. The trajectories of the randomly chosen nucleons facing minimal (left panel) and maximal (right) collisions followed for the time span of 300 fm/c. The calculations are shown in the x - z plane for the single event of Ca (400 AMeV)+ Ca collision, with $b/b_{max}=0.3$.

- 162 245; Kumar S, Puri R K and Aichelin J 1998 Phys. Rev. C **58** 1618; Gossiaux P B, Puri R K, Hartnack Ch, Aichelin J 1997 Nucl. Phys. A **619** 379.
- [20] Huang S W et al 1993 Phys. Lett. B **298** 41; Huang S W et al 1993 Prog. Part. Nucl. Phys. **30** 105.
- [21] Batko G et al 1994 J. Phys. G: Nucl. Part. Phys. **20** 461.
- [22] Khoa D T et al 1992 Nucl. Phys. A **619** 102 (1992); Puri R K et al 1994 Nucl. Phys. A **575** 733.
- [23] Braun-Munzinger P, Stachel J, Wessels J P and Xu N 1996 Phys. Lett. B **365** 1; Braun-Munzinger P, Heppel I and Stachel J 1999 Phys. Lett. B **465** 15.
- [24] Andronic A, Braun-Munzinger P and Stachel J 2006 Nucl. Phys. A **772** 167.
- [25] Sehn L and Wolter H H 1990 Nucl. Phys. A **519** 289
- [26] Shi L, Danielewicz P and Lacey R 2001 Phys. Rev. C **64** 034601
- [27] Pochodzalla J et al 1995 Phys. Rev. Lett. **75** 1040
- [28] Schüttauf A et al 1996 Nucl. Phys. A **607** 457
- [29] Gaitanos T, Wolter H H and Fuchs C 2000 Phys. Lett. B **478** 79
- [30] Doss K G R et al 1988 Phys. Rev. C **37** 163
- [31] Haddad F, Natowitz J B, Jouault B, Mota V de la, Royer G and Sébille F 1996 Phys. Rev. C **53** 1437
- [32] Liu J Y, Guo W J, Xing Y Z, Zuo W and Lee X G 2003 Phys. Rev. C **67** 024608
- [33] Vermani Y K and Puri R K 2009 J. Phys. G: Nucl. Part. Phys. **36** 105103
- [34] Chomaz Ph, Lacroix D, Jacquot B, Colonna M and Ayik S 1999 International Workshop on the Gross Properties of Nuclei and Nuclear Excitations, Hirschegg, Austria, p 312-321.
- [35] Liu J Y and Zhang S G 1994 Z. Phys. A **348** 31
- [36] Chomaz Ph and Hasnaoui K H O arXiv:nucl-th/0610027
- [37] Aichelin J 1991 Phys. Rep. **202** 233
- [38] Lehmann E, Puri R K, Faessler A, Batko G and Huang S W 1995 Phys. Rev. C **51** 2113
- [38] Hartnack Ch et al 1998 Eur. Phys. J. A **1** 151; Singh J, Kumar S and Puri R K 2000 Phys. Rev. C **62** 044617.
- [39] Kumar Sanjeev, Kumar S and Puri R K 2008 Phys. Rev. C **78** 064602; Kumar Sanjeev, Kumar S and Puri R K 2010 Phys. Rev. C **81** 014611; Kumar Sanjeev, Kumar S and Puri R K 2010 Phys. Rev. C **81** 014601; Gautam S, Chugh R, Sood A D, Puri R K, Hartnack Ch and Aichelin J 2010 J. Phys. G: Nucl. Part. Phys. **37** 085102.
- [40] Doss K G R et al 1985 Phys. Rev. C **32** 116
- [41] Gutbrod H H, Poskanzer A M and Ritter H G 1989 Rep. Prog. Phys. **52** 1267
- [42] Stöcker H and Greiner W 1989 Phys. Rep. **52** 1267; Siemens P J and Rasmussen J O 1979 Phys. Rev. Lett. **42** 880.